NANO LETTERS

2007
Vol. 7, No. 12
3623−3627

Reversible Defect Engineering of Single-Walled Carbon Nanotubes Using Scanning Tunneling Microscopy

Maxime Berthe,[†,||] Shoji Yoshida,[†] Yuta Ebine,[†] Ken Kanazawa,[†] Arifumi Okada,[†] Atsushi Taninaka,[†] Osamu Takeuchi,[†] Nobuyuki Fukui,[‡] Hisanori Shinohara,[‡] Satoru Suzuki,[§] Koji Sumitomo,[§] Yoshihiro Kobayashi,[§] Bruno Grandidier,[||] Didier Stiévenard,[||] and Hidemi Shigekawa*,[†]

Institute of Applied Physics, Crest, University of Tsukuba, Tsukuba, 305-8573, Japan, Department of Chemistry, Nagoya University, Nagoya, 464-86,2, Japan, NTT Basic Research Laboratories, NTT Corporation, Atsugi, Kanagawa 243-0198, Japan, and Institut d'Electronique, de Microélectronique, et de Nanotechnologie, IEMN (CNRS, UMR 8520), Département ISEN, 41 bd Vauban, 59046 Lille Cédex, France

Received July 28, 2007; Revised Manuscript Received October 15, 2007

ABSTRACT

The experimental creation and annihilation of defects on single-walled carbon nanotubes (SWCNT) with the tip of a scanning tunneling microscope are reported. The technique used to manipulate the wall structure of a nanotube at the atomic scale consists of a voltage ramp applied at constant tunneling current between the tip and the nanotube adsorbed on a gold substrate. While topographic images show an interference pattern at the defect position, spatially resolved tunneling spectroscopy reveals the presence of localized states in the band gap of the nanotube. Removal of the defect by the same procedure demonstrates the reversibility of the process. Such a precise control in the local modification of the nanotube wall opens up new opportunities to tailor SWCNT electronic properties at will.

Owing to their unique aspect ratio, single-walled carbon nanotubes (SWCNTs) have attracted considerable attention in the study of transport across one-dimensional systems.[1] The way they are wrapped not only determines their geometric properties but also their electronic structure: semiconductive or metallic. Such properties allow SWCNTs to be used as functional devices like transistors.[2] Recent studies have focused on the engineering of SWCNT properties such as the exploitation of intramolecular junctions[3] or the modification of their band gap by the insertion of impurities: ions[4] or molecules.[5] Atomic defects are also investigated as good candidates for tailoring the electronic properties of SWCNTs; for example, Lee et al. observed deep and shallow levels associated with vacancy-adatom and pentagon-heptagon defects,[6] and Park et al. modulated the electron transmission probability of a defect by an electric field.[7] Until now, several types of defects, like Stone-Wales defects,[8] vacancies,[9] ad-dimers,[10] or H−C complex[11] could be introduced on SWCNTs by electron or ion sputtering.[9,11,12] But the incorporation of defects in the nanotube generally relies on macroscopic processes, which inherently involve the creation of several defects in the same nanotube with a large dispersion on their spatial distribution. Therefore no precise control of the creation or even removal of defects in a single nanotube has been achieved so far.

Because of the nanometer size of SWCNTs, scanning tunneling microscopy (STM) is a quite suitable technique for the investigation of the SWCNTs properties.[13] It has been widely used to study their electronic structure as well as identify and characterize individual defects on their surface.[14] More remarkably, it can also be used to manipulate SWCNT by locally cutting the tube for example.[15] But to date this technique has not yet been proved to tailor the properties of SWCNTs without destroying them.

In this paper, we describe a method to selectively modify the electronic properties of semiconductor SWCNTs by the creation and destruction of point defects on their surface with an STM tip. The fabrication of the defects is detected from the measurements of the tip height variation when the sample voltage is increased to a few volts maintaining the tunneling current constant. The investigation of the defect nature by STM topographic images shows the formation of interference patterns on the nanotube wall, and spatially tunneling spectroscopic measurements reveal that this pattern is related

* Corresponding author. Website: http://dora.ims.tsukuba.ac.jp.
[†] University of Tsukuba.
[‡] Nagoya University.
[§] NTT Corporation.
[||] IEMN (CNRS, UMR 8520).

10.1021/nl071845c CCC: $37.00
Published on Web 11/23/2007

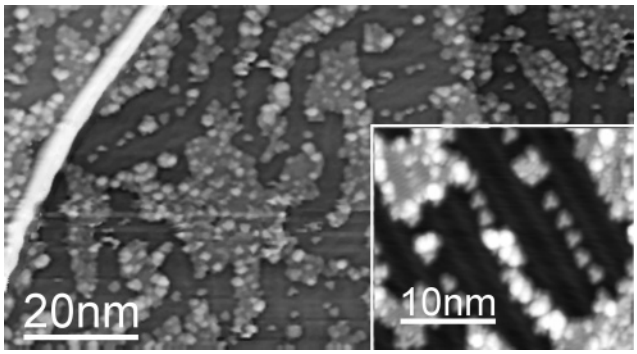

Figure 1. STM image of SWCNT deposited by spin coating on a freshly cleaned Au(111) surface (sample voltage $V_s = -1$ V, tunneling current setpoint $I_t = 100$ pA, $T = 4$ K). Inset: High-resolution STM image of a smaller area partially covered with molecular species from the solvent ($V_s = 1.0$ V, $I_t = 100$ pA, $T = 4$ K).

to the presence of localized states in the band gap of the nanotube. Because the defects are removed by applying a similar voltage ramp, the controlled formation of localized states in the band gap of the nanotube indicates that the atomic scale modification of its electronic structure is fully reversible, providing new pathways to tailor SWCNT electronic properties.

The experiments were conducted with an Omicron LT-STM operated at 77 and 4 K on SWCNTs deposited by spin coating on freshly prepared and flame-annealed Au(111) samples. We used electrochemically etched PtIr and W tips, cleaned in ultrahigh vacuum (UHV) by heating and electron bombardment. HiPCO[16] SWCNTs dissolved in chloroform and 1-2-dichloroethane were used at a concentration of 1 μg/10 mL. Then the solution was ultrasonicated for more than 1 h to obtain individual nanotubes. After ultrasonication, one drop was deposited by spin coating on the freshly cleaned Au(111) sample. The samples were then introduced into UHV and degassed before the experiments.

Figure 1 shows a large scale STM image obtained after the deposition of SWCNTs on a Au(111) surface. A SWCNT is clearly visible on the left of the image, running along the edge of an atomic terrace. We note that the terraces are partially covered with molecules from the solvent. The observation of single molecules self-aligned in the face-centered cubic region of the herringbone reconstruction in the inset of Figure 1 reveals a ternary symmetry, suggesting the adsorption of chloroform molecules of the solvent during the deposition of SWCNTs.

After having identified the geometric properties of a CNT from its wrapping angle and its energy gap (for semiconducting CNTs) or low-conductivity zone (for metallic CNTs) based on established procedures,[17] the STM tip was immobilized on a defect-free location on the SWCNT. The creation of protrusions on the nanotube wall was then performed using the method described in Figure 2. A voltage ramp was additionally applied on the sample voltage used to image a SWCNT, as shown by the curve labeled V_s. The typical sweep time was 0.1 s/V. During the voltage ramp, the feedback loop was kept closed and as a result, the tip−sample distance Z increased to keep the tunneling current I_t

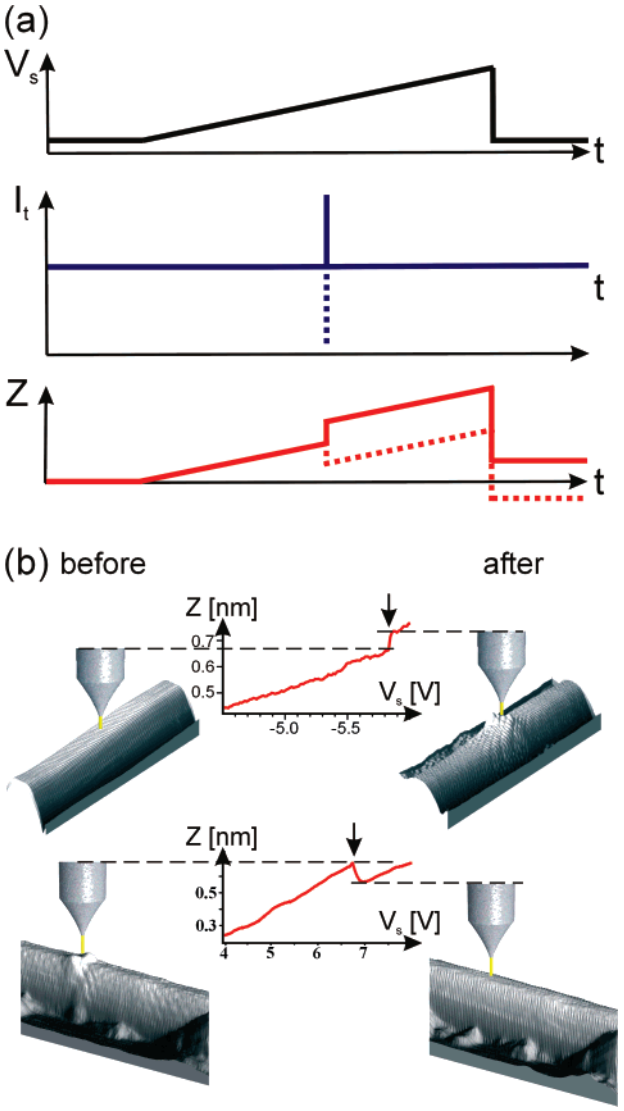

Figure 2. (a) Experimental scheme used to create a defect on a SWCNT. The STM tip is first immobilized over a defect-free position at the surface of a SWCNT. While maintaining the feedback loop close (I_t constant), the sample voltage V_s is usually ramped up to ±8 V and both I_t and the tip height Z variation are recorded. At the time of the defect creation or annihilation, a sharp peak occurs on the tunneling current as well as a sudden shift of the tip height, away from the surface for the creation (continuous line), closer to the surface for the annihilation (dotted line). (b) STM images of a SWCNT before and after the defect creation (top) or annihilation (bottom) along with a portion of the experimental $Z(V)$ curves showing a sudden shift of the tip height (vertical arrow), signature of the defect creation or annihilation (Feedback parameters: $V_s = -0.4$ V, $I_t = 200$ pA, $T = 4$ K).

constant. At certain bias, a sharp step appeared on Z indicating an additional backward shift of the tip from the nanotube. This step is the response of the piezo controlling the tip height to a sudden increase in the tunneling current while the sample voltage increases. After the voltage sweep, the tip started again scanning the nanotube. Figure 2b shows the modification of the nanotube when a negative sample voltage ramped is applied to a defect-free SWCNT. At a voltage of −5.8 V, an abrupt change in the linear behavior of the $Z(V)$ curve occurs. After this event, a deformation on

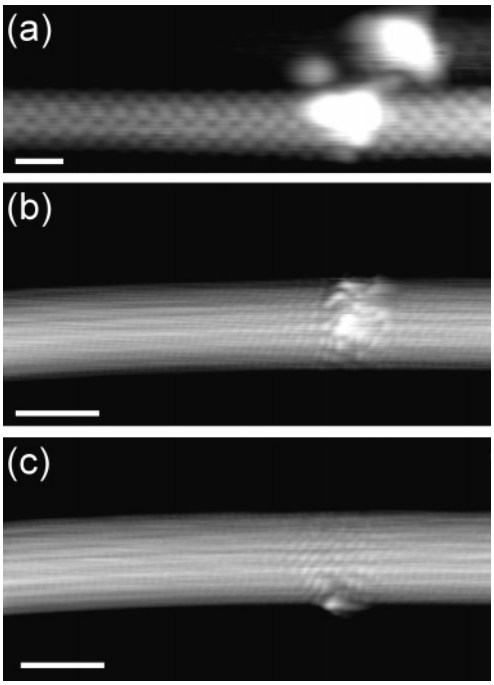

Figure 3. Examples of protrusions created by the tip and observed on the nanotube wall in topographic STM images. Protrusions are divided in (a) type A protrusions associated with adsorbates (V_s = 1.0 V, I_t = 200 pA, and (b,c) type B protrusions associated with point defects. (V_s = −0.5 V/−0.8 V, I_t = 100 pA). Scale bar: 1 nm.

the nanotube wall was clearly visible at the position where the voltage ramp was performed.

Similarly, applying a voltage ramp at constant current on a protrusion created by the tip leads to the annihilation of the protrusion and restores the defect-free structure of the nanotube wall, as shown in Figure 2. We note that the voltage threshold required to modify the nanotube varies and that multiple events can sometimes occur in a single voltage ramp, indicating both the creation and removal reactions during the same voltage ramp.

The protrusions, which are created by this method, exhibit different shapes that are visible in Figure 3. They can be divided in two categories: protrusions that show an unperturbed structure of the nanotube lattice surrounding the protrusion (type A) and protrusions which involve strong distortion of the nanotube lattice (type B). An example of type A protrusion is seen in Figure 3a, and we associated it with the adsorption of a molecule onto the wall of the nanotube.[18] This molecule may diffuse from the Au(111) surface to adsorb on the nanotube or may have been picked up by the tip during scanning and is released on the nanotube during the voltage ramp. In contrast, type B protrusions show a lower contrast (see Supporting Information, Figure S4), and the protrusions resemble those generally attributed to point defects in the nanotube.[6,14] They are found either on top of the nanotube (Figure 3b) or on the sidewall (Figure 3c). As the interference pattern observed for these protrusions suggests an electronic origin with the expectation of a strong modification of the local density of states at the position of the defect, we focus the rest of the paper onto type B protrusions.

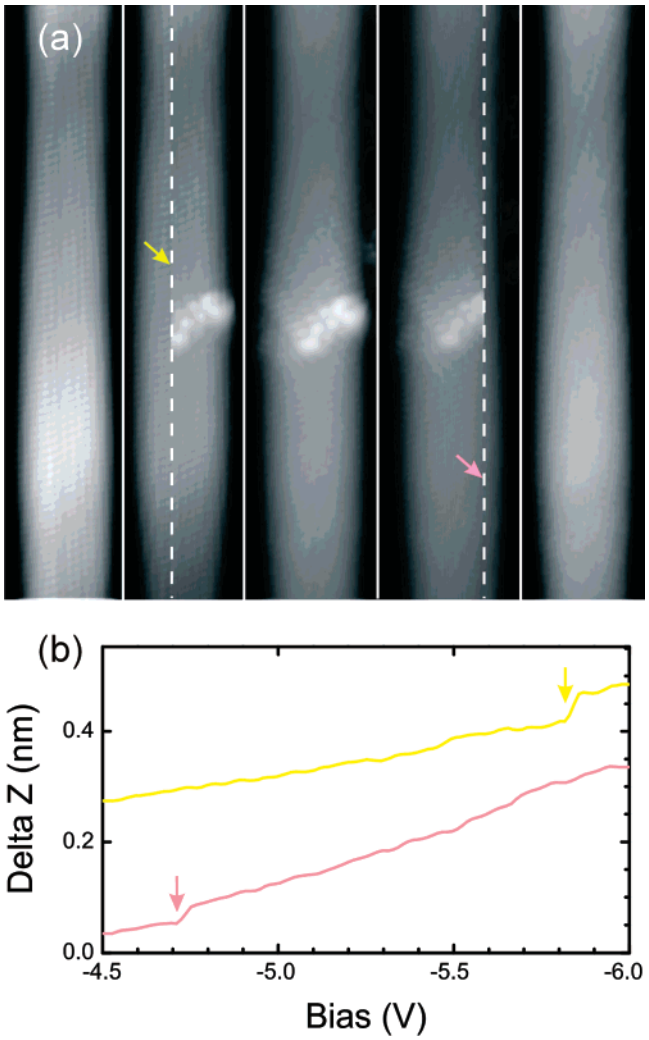

Figure 4. (a) From left to right: series of successive STM topography images (5 × 16 nm^2, V_s = −0.4 V; I_t = 200 pA) taken at T = 4 K at the same place on a (9,5) CNT before the creation of a defect, during the creation of the defect, with the created defect, during the removal of the defect, and after the annihilation of the defect. The scan direction for each image is from right to left. The dashed lines and the arrows indicate, respectively, when and where the voltage ramp was applied during scanning. (b) Portion of $Z(V)$ curves showing the characteristic step, indicated by a vertical arrow, and related to the local modification of the SWCNT. The upper curve corresponds to the voltage ramp used for the creation of the defect, and the lower one is for its annihilation.

Central to the work reported here is our ability to create and subsequently remove a type B protrusion. An example is given in Figure 4, where a defect-free nanotube is first imaged and the voltage ramp is then turned on (upper curve in Figure 4b). After the voltage is reset to its initial value, a protrusion is visible in the middle of the nanotube. By applying a second voltage ramp to the nanotube, the protrusion disappears. Although the characteristic step in the $Z(V)$ curve does not occur at the same voltage used for the creation of the protrusion (lower curve in Figure 4b), the nanotube recovers its initial crystallographic structure, as shown in the last STM image of Figure 4a. Interestingly, the example in Figure 4 illustrates that the creation or removal of a defect does not always occur at the position

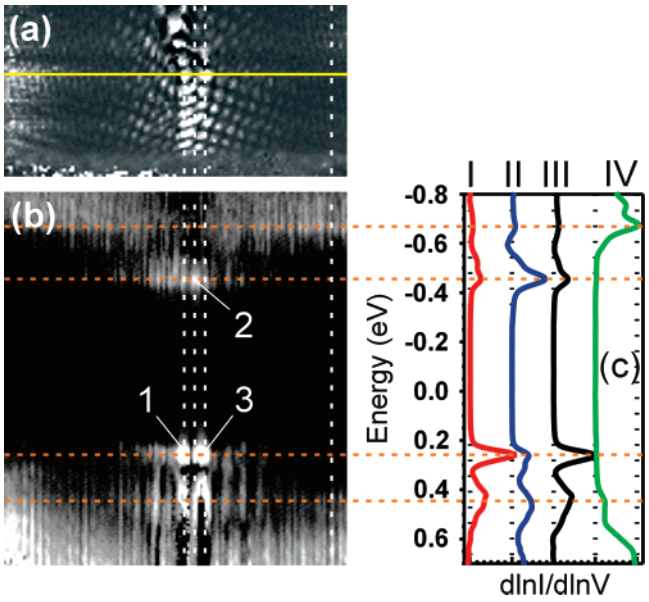

Figure 5. (a) dI/dV image acquired at $V_s = +0.4$ V in the region of the defect shown in Figure 4. The image is rotated by 90° with respect to the STM images of Figure 4. Feedback parameters $V_s = -0.9$ V, $I_t = 200$ pA, $T = 4$ K. Image size: 10 nm × 5 nm. (b) Spatial variation of dI/dV as a function of the sample voltage acquired along the horizontal line in panel a. The four horizontal dashed lines indicate characteristic energy positions in the dI/dV curves: the upper and lower ones correspond to the band gap of the nanotube and the line in between corresponding to the defect states (areas 1, 2, and 3). (c) dI/dV curves corresponding respectively to the four vertical dashed lines running through the defect states (I−III from left to right) and a defect-free region (IV, upmost to the right) in panels a,b.

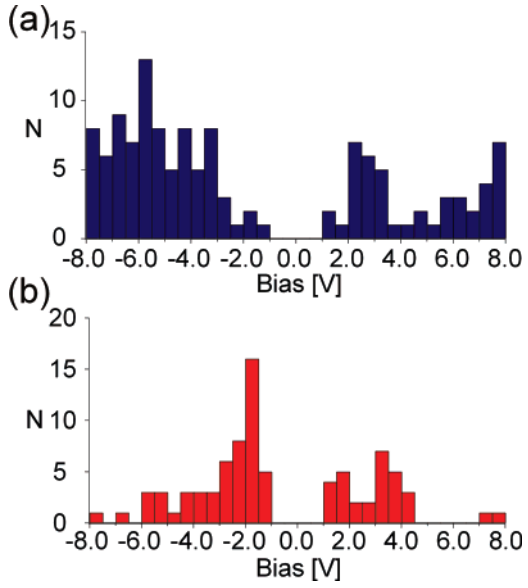

Figure 6. Distribution of the voltage thresholds for (a) creation and (b) annihilation events.

where the voltage sweep is applied, but a few nanometer apart. In that case, the annihilation of the defects might take place with a backward step of the Z piezo, instead of a decrease of the tip−sample distance as shown in Figure 2b.

Because the lattice distortion is likely to be caused by a local modification of the nanotube electronic structure, spatially resolved spectroscopic measurements were performed on the nanotube shown in Figure 4 between the creation and annihilation processes. Figure 5a shows the differential conductance imaged at 0.4 V in the area of the defect, where an interference pattern is clearly seen wrapping the nanotube, but spatially localized along the main axis of the nanotube. To get a better insight into the local variation of the SWCNT electronic structure, the variations of the differential conductance are plotted as a function of the voltage along a line running through the defect. As seen in Figure 5b, while the band gap of the nanotube is measured to be 1.13 eV in the defect-free region deduced from most external horizontal dashed lines, the dI/dV profile measured on the defect clearly shows intense signal in the band gap region of the nanotube at energies of at −0.45 and +0.26 eV. Those peaks, visible in Figure 5c, are quite localized along the main axis of the nanotube and are consistent with the position of the deep levels generally found for point defects related to vacancy-adatom pair or adatom−adatom complex in a nanotube.[6,19,20] Although theoretical support is required to determine the precise nature of the defect created on this (9,5) nanotube, the spectroscopic measurements indicate that the creation of a type B protrusions causes a significant modification of the nanotube electronic structure, spatially localized at the location of the defect.

We have observed that the type B protrusions are stable for days if we do not apply a second voltage sweep to the nanotube and that it did not disappear due to thermal fluctuations event at room temperature. To further understand the creation and annihilation reaction discussed above, we examined the bias-voltage dependence of the reaction rates. For this purpose, the voltage ramps were applied on many nanotubes with different STM tips. The sample voltage was swept from ±1.0 to ±8.0 V with increasing absolute value of V_s in 1.2 s. During the voltage ramp, the tip−sample distance was feedback controlled with the reference tunnel current at 1.0 nA. All experiments were performed at 77 K. The histograms of the sample voltage thresholds at which the creation or annihilation events occur are shown in Figure 6.

The distribution of the voltage thresholds for the creation events does not mark a clear onset, although the creation of a defect is lower for smaller voltages. Conversely, the probability to produce an annihilation event is the highest at small voltages indicating therefore that the energy barrier height for the annihilation process is lower than the one for the creation process. Futhermore, it is worth pointing out that the measured voltage thresholds are smaller compared with the barrier energy for the removal of a carbon atom from a SWCNT, which was estimated to be 10 to 20 eV.[21] Usually, for an accelerated electron to give this amount of energy to a CNT, electrons must be accelerated up to 100 keV.[21] In contrast, the amount of energy needed to rotate a C−C bond in a nanotube wall or to create a point defect induced by a hydrogen ion is found to be compatible with the range of voltage thresholds shown in Figure 6.[22,23] Although we cannot rule out that hydrogen ions may be produced by the voltage ramp due to their desorption from

molecular species in the vicinity of the nanotube and their further adsorption on the nanotube wall, the reproducibility of the defect shape for several successive creation events on the same nanotube favors the formation of defects related to the rotation of C−C bonds (see Supporting Information). Variability of the threshold voltages is also consistent with the variation of the energy barrier to create or annihilate point defects induced by different rotation of C−C bonds, whose formation energy depends on the helicity of the nanotubes.[24]

In a conclusion, we propose a method to form point defects on the wall of a nanotube based on the application of a voltage ramp while the tunneling current is kept constant between the STM tip and the nanotube. The defects show localized states in the band gap of the nanotube, and spectroscopic studies as well as the analysis of the energetic distribution for the defect formation suggest the creation of defects induced by the rotation of C−C bonds, such as Stone-Wales defects. Remarkably, the defects are removed by the same methods, allowing the nanotube wall to recover its initial structure. Such a reversible manipulation of the nanotube wall should open the way to create confined regions within SWCNTs.

Acknowledgment. This work was supported in part by a Grant-in-Aid for Scientific research from the Ministry of Education, Culture, Sports, Science, and Technology of Japan.

Supporting Information Available: Figures showing different sequences of creation and annihilation events. This material is available free of charge via the Internet at http://pubs.acs.org.

References

(1) (a) Iijima, S. *Nature* **1991**, *354*, 56. (b) Saito; R.; Fujita; M.; Dresselhaus, G.; Dresselhaus, M. S. *Appl. Phys. Lett.* **1992**, *60*, 2201. (c) Hamada, N.; Sawada, S. I.; Oshiyama, A. *Phys. Rev. Lett.* **1992**, *68*, 1579. (d) Tans, S. J.; Devoret, M. H.; Dai, H.; Thess, A.; Smalley, R. E.; Geerligs, L. J.; Dekker, C. *Nature* **1997**, *386*, 474.
(2) Tans, S. J.; Verschueren, A. R. M.; Dekker, C. *Nature* **1998**, *393*, 49.
(3) Yao, Z.; Postma, H. W. Ch.; Balents, L.; Dekker, C. *Nature* **1999**, *402*, 273.
(4) Zhou, C.; Kong, J.; Yenilmez, E.; Dai, H. *Science* **2000**, *290*, 1552.
(5) Lee, J.; Kim, H.; Kahng, S. J.; Kim, G.; Son, Y. W.; Ihm, J.; Kato, H.; Wang, Z. W.; Okazaki, T.; Shinohara, H.; Kuk, Y. *Nature* **2002**, *415*, 1005.
(6) Lee, S.; Kim, G.; Kim, H.; Choi, B. Y.; Lee, J.; Jeong, B. W.; Ihm, J.; Kuk, Y.; Kahng, S. J. *Phys. Rev. Lett.* **2005**, *95*, 166402.
(7) Park, J.-Y. *Appl. Phys. Lett.* **2007**, *90*, 023112.
(8) Stone, A. J.; Wales, D. J. *Chem. Phys. Lett.* **1986**, *128*, 501.
(9) Smith, B. W.; Luzzi, D. E. *J. Appl. Phys.* **2001**, *90*, 3509.
(10) Orlikowski, D.; Nardelli, M. B.; Bernholc, J.; Roland, C. *Phys. Rev. Lett.* **1999**, *83*, 4132.
(11) Nikitin, A.; Osagawara, H.; Mann, D.; Denecke, R.; Zhang, Z.; Dai, H.; Cho, K.; Nilsson, A. *Phys. Rev. Lett.* **2005**, *95*, 225507.
(12) Krasheninnikov, A. V.; Nordlund, K.; Keinonen, J. *Phys. Rev. B* **2002**, *65*, 165423.
(13) (a) Wildöer, J. W. G.; Venema, L. C.; Rinzler, A. G.; Smalley, R. E.; Dekker, C. *Nature* **1998**, *391*, 59. (b) Odom, T. W.; Huang, J.-L.; Kim, P.; Lieber, C. M. *Nature* **1998**, *391*, 62.
(14) Ishigami, M.; Choi, H. J.; Aloni, S.; Louie, S. G.; Cohen, M. L.; Zettl, A. *Phys. Rev. Lett.* **2004**, *93*, 196803.
(15) Rubio, A.; Apell, S. P.; Venema, L. C.; Dekker, C. *Eur. Phys. J. B* **2000**, *17*, 301.
(16) Martell, R.; Schmidt, T.; Shea, H. R.; Hertel, T.; Avouris, Ph. *Appl. Phys. Lett.* **1998**, *73*, 2447.
(17) Venema, L. C.; Meunier, V.; Lambin, Ph.; Dekker, C. *Phys. Rev. B* **2000**, *61*, 2991.
(18) Graupner, R.; Abraham, J.; Wunderlich, D.; Vencelova, A.; Lauffer, P.; Röhrl, J.; Hundhausen, M.; Ley, L.; Hirsch, A. *J. Am. Chem. Soc.* **2006**, *128*, 6683.
(19) Kim, H.; Lee, J.; Lee, S.; Kuk, Y.; Park, J.-Y.; Kahng, S. J. *Phys. Rev. B* **2005**, *71*, 235402.
(20) Buchs, G.; Krasheninnikov, A. V.; Ruffieux, P.; Gröning, P.; Foster, A. S.; Nieminen, R. M.; Grönnig, O. *New. J. Phys.* **2007**, *9*, 275.
(21) Banhart, F. *Rep. Prog. Phys.* **1999**, *62*, 1181.
(22) Nardelli, M. B.; Yacobson, B. I.; Bernholc, J. *Phys. Rev. B* **1998**, *57*, R4277.
(23) Buchs, G.; Ruffieux, P.; Gröning, P.; Grönnig, O. *Appl. Phys. Lett.* **2007**, *90*, 013104.
(24) Zhou, L. G.; Shi, S.-Q. *Appl. Phys. Lett.* **2003**, *83*, 1222.

NL071845C